C 80-087

Unsteady Stator Response to Upstream Rotor Wakes

20009
20016

G.F. Franke* and R.E. Henderson†
Pennsylvania State University, University Park, Pa.

The results are presented of an investigation of the unsteady pressures generated on a stator due to its interaction with the wakes shed by an upstream rotor. The influence of stator solidity, incidence flow angle, and rotor-stator spacing are discussed. The results show a major influence due to stator solidity at large values of incidence angle where it is suspected that stall occurred. Comparisons of the measured data with an existing unsteady cascade analysis show similar trends in the chordwise variation of the predicted and measured unsteady pressure difference across the blades. Comparisons with an isolated airfoil analysis indicate the influence of solidity and unsteady blade-to-blade interaction. All comparisons were conducted for an incompressible flow with a reduced frequency of approximately 5.0.

Nomenclature

BPF	= blade passing frequency
c	= chord length
C_N	= Fourier modulus
$\tilde{C}_p$	= unsteady pressure coefficient
$C_{p_{\text{rms}}}$	= unsteady pressure coefficient, rms
i	= angle of incidence
$\tilde{p}$	= unsteady pressure
p_{atm}	= atmospheric pressure
R/S	= rotor-stator axial spacing
r	= radius
s	= blade spacing
t	= time
T_0'	= nondimensional time
U	= rotor blade speed
u_d	= wake deficit parallel to chord
V	= absolute velocity (relative to stator)
v_d	= wake deficit normal to chord
W	= relative rotor velocity
w_d	= wake deficit
x	= distance from along chord from leading edge
α	= absolute flow angle
β	= relative flow angle
ξ	= stagger angle
ρ	= density
σ	= solidity
ϕ	= phase angle
ω	= reduced frequency

Subscripts

m	= mean
N	= Fourier harmonic
R	= rotor
S	= stator
x	= axial
2	= rotor exit or stator inlet

Presented as Paper 79-0579 at the AIAA 5th Aeroacoustics Conference, Seattle, Wash., March 12-14, 1979; submitted April 24, 1979; revision received Dec. 26, 1979.

Index categories: Nonsteady Aerodynamics; Subsonic Flow.

*Graduate Assistant, Department of Mechanical Engineering and Applied Research Laboratory; presently at Hydro-Turbine Division, Allis-Chalmers Corporation, York, Pa.

†Professor, Department of Mechanical Engineering and Applied Research Laboratory. Member AIAA.

Introduction

APART of the noise generated in an axial flow fan stage results from the interaction of the wakes from the blades of an upstream rotor and a downstream stator.[1] As a result of this interaction and the relative motion of the wakes with respect to the stator blades, unsteady forces and pressures are generated on the stators which contribute to the noise tones radiated by the fan stage. Thus, an important factor in the design of advanced fan stages is the reduction of the unsteady forces and pressures generated on the stators.

To achieve a reduction in the stator generated noise tones in an advanced fan stage, it is necessary for the designer to have a knowledge of the variation of the unsteady forces and pressures on the stators as a function of the characteristics of the wakes and the stator design variables. In this way, a stator configuration can be selected which will result in a minimum unsteady response and, hence, radiated noise. The design variable which the designer can consider include: 1) the reduced frequency of the disturbance or wakes ω; 2) the solidity of the stator σ; 3) the angle of incidence i of the time-mean flow at the stator inlet; 4) the stagger angle of the stator blades ξ_s; and 5) the axial spacing between the trailing edge of the rotor and the leading edge of the stator (R/S).

Several attempts to determine optimum fan stage stator configurations have been reported. Dittmar[2] employed an unsteady isolated airfoil analysis based on the methods reported by Sears[3] and Horlock[4] and considered all of the aforementioned effects except stator solidity. The results of this study were employed in the redesign of a fan stage. The evaluation of this redesigned fan[5] showed very little improvement in the noise tones and no where near the predicted improvement. This result was attributed to the complexity of the experiment and the fact that flow distortions other than the rotor wakes may have been present which controlled the tone noise. A recent analysis by Goldstein and Atassi[6] suggests that the Horlock analysis used by Dittmar is incorrect. This may explain the lack of measured improvement reported in Ref. 5.

Henderson[7] has reported the results of theoretical predictions of the unsteady lift on a cascade of airfoils which includes all of the above effects except the rotor-stator axial spacing. These predictions indicate a major influence due to the cascade solidity for values of reduced frequency less than 3.0 or when the blade spacing is nearly equal to the disturbance wavelength.

The present study was conducted to provide further experimental data to demonstrate the influence of rotor-stator spacing, stator solidity, and steady loading (incidence angle) on the unsteady pressures generated on a stator blade row operated in the wakes of an upstream rotor at a reduced frequency of approximately 5.0. Distributions of the unsteady

pressures on both the suction and pressure surfaces of an unstagger stator blade row were measured and compared with existing theoretical analyses by Meyer[8] for an isolated airfoil and by Whitehead[9] and Smith[10] for a cascade of airfoils. Other investigations of unsteady pressure distributions in a cascade of airfoils include those by Satyanayarana[11] and Ostdiek.[12] However, these studies employed a stationary two-dimensional cascade and operated with nonconvected disturbances.

Experimental Apparatus and Instrumentation

Axial Flow Research Fan

The Axial Flow Research Fan (AFRF), located in the Applied Research Laboratory, was employed for this study. The AFRF[13] consists of a bellmouth inlet leading to an annular flow passage with a 54.61-cm o.d. and a 24.13-cm i.d., and contains the test rotor and stator together with an auxiliary fan which provides the airflow through the annulus. For this study, the through flow velocity was approximately 19.8 m/s and the rotor tip speed approximately 115 m/s.

The rotor employed 12 blades having a 10% thick uncambered C1 thickness profile, a chord length of 15.24 cm, and a span of 14.99 cm. The rotor blades were twisted to have a zero angle of incidence at all blade radii at the design condition and a rotor stagger angle ξ_R of 45 deg at the mean radius. The rotor and auxiliary fan drive motors can be independently operated by variable frequency motor and power supplies. The stator incidence angle was varied by changing the rotor rpm and, consequently, the stator inlet fluid angle.

The test stator consisted of either 4 or 8 blades having the same cross-sectional shape as the rotor blades and positioned to give rotor-stator spacings of 0.5 or 2.0 rotor chord lengths. This spacing was measured as the axial distance from the rotor trailing edge to the stator leading edge. The stator blades were untwisted and had a constant stagger angle of 0 deg. Two of the stator blades were instrumented to measure the unsteady pressures $\tilde{p}$ on the blade surface. A blade chord Reynolds number of approximately 2×10^5 was employed throughout the study.

A once-per-rotor revolution signal was produced to indicate the position of the rotor in each revolution and permitted the accurate tracking of data produced during different rotor revolutions.

Instrumented Stator

Two of the stator blades were instrumented to measure the unsteady surface pressures. One blade contained six transducers located at 5, 15, 30, 40, 50, and 75% of the chord. The second blade contained transducers at the 2, 40, and 95% chord locations.

Each instrumented stator blade consisted of two sections which fit together to form internal cavities in which the pressure transducers were mounted. The transducers were mounted between a pair of o-rings as shown in Fig. 1. The dimensions of the internal cavities and surface taps were selected to minimize cavity resonance effects, and the surface taps were staggered about the mean radius ($r_m = 19.68$ cm) in a manner to cover a spanwise extent of approximately 2.5 cm. To measure pressures on the pressure surface of a blade, the holes on the suction surface were covered with tape, and vice versa.

The transducers employed were Pitran model PT-M2 differential pressure transducers manufactured by Stow Laboratories. The Pitran is a silicon NPN planar transistor with the emitter-base junction mechanically coupled to a diaphragm. These transducers were selected because of the following characteristics: 1) linear output over the rated pressure range (0.25 psid), 2) high output signal voltage of approximately 1 V per cm of water of applied pressure, 3) a resonant frequency greater than 100,000 Hz, 4) a maximum diameter of 0.5 cm, and 5) large overload capability of approximately 700% of rated pressure without damage.

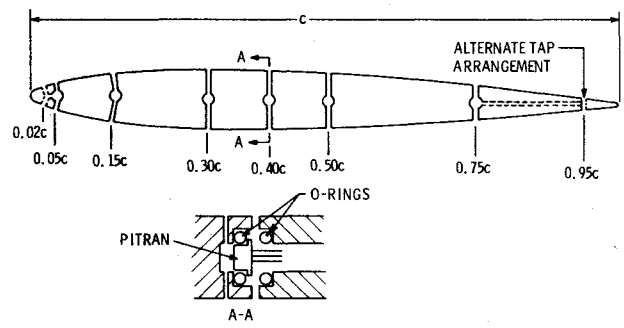

Fig. 1 Instrumented stator cross section and transducer mounting.

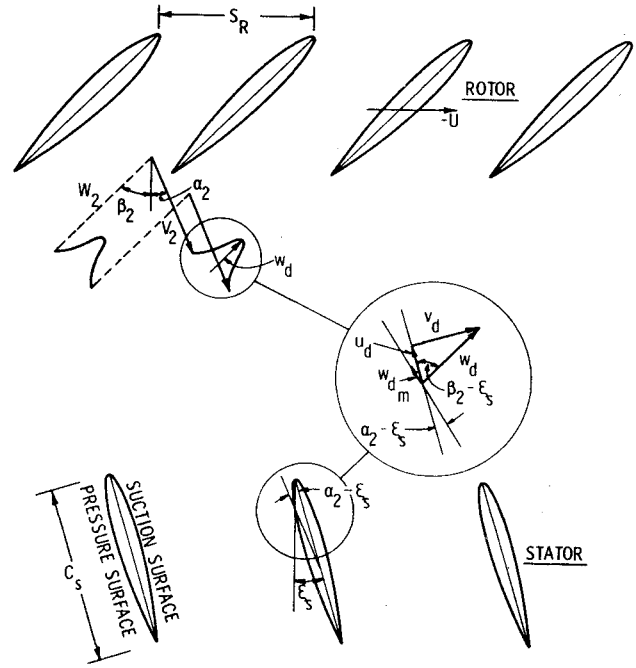

Fig. 2 Definition of wake velocity deficit.

Flowfield Instrumentation

Measurements were made of pertinent flow field characteristics at the leading edge of the stators. These included the axial velocity V_x, the resultant absolute velocity V and the velocity deficit by the viscous rotor wakes w_d (see Fig. 2).

A three-hole probe was positioned at the mean radius approximately 3 cm upstream of the stator to determine the time-mean flow angle α_2. A hot-film anemometer probe was then located at the mean radius, aligned normal to the absolute flow direction, and used to determine the velocity profile of the rotor wake.

Both the three-hole and hot-film probes were located circumferentially between the stator blades to minimize the effect of the probe wake on the instrumented blades. As the rotor-stator spacing was changed, the hot-film probe was maintained at a position as close as possible to the leading edge of the stator, thus recording the rotor wake characteristics that most nearly represent the rotor wake at the stator leading edge.

Instrumentation of Signal Conditioning

The Pitran signal was conditioned by a Stow Laboratories model 861 Signal Conditioner which continuously compensated for the response to very low-frequency variations of pressure and temperature. The output of each transducer was recorded on magnetic tape.

The signals of several of the Pitrans were contaminated by a large 60-Hz component. Since the Pitran output contained no significant information near this frequency [the lowest rotor

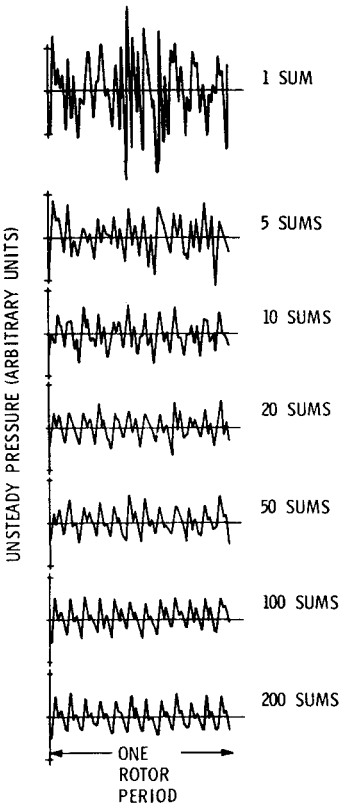

Fig. 3 Effect of ensemble-averaging on transducer signal.

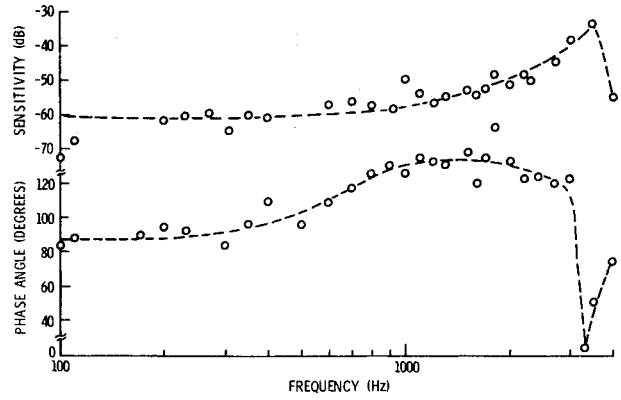

Fig. 4 Dynamic response of transducer at $x/c = 0.15$.

blade passing frequency (BPF) was 200 Hz], a high-pass filter set at 80 Hz was used on all signals to eliminate the 60-Hz signal. To account for the frequency-dependent phase shift introduced by the filters, the ensemble-averaged signal from each sensor was Fourier analyzed and corrected by an appropriate amount.

As the data were being recorded, the signal from each terminal of the tape recorder was analyzed with a Spectral Dynamics Real Time Analyzer Model SD301C to determine the signal output as a function of frequency. This ensemble-averaged frequency spectrum provided a useful check that the data acquisition system was functioning properly.

After recording the time-dependent signals from the sensors on magnetic tape, the data were analyzed with an IBM System 7 real-time computer programmed to perform an ensemble-average of the data in the time domain. This technique enhanced the portion of the signal that was periodic with respect to the once-per-revolution pulse and eliminated the non-periodic signal caused by turbulent fluctuations, electronic noise, or a response to events not related to the wake/stator interaction. Figure 3 shows the effect on the output of a typical Pitran of different numbers of sums or rotor revolutions. Two hundred sums were used for all of the final data.

Calibration of Instrumented Stators

The instrumented stators were assembled and dynamically calibrated prior to their installation in the AFRF. In addition, the assembled blades were installed in a pressure test chamber in which a steady pressure differential was applied across each transducer to check the sealing and installation of each transducer.

Since the Pitran transducers were mounted in a tube/cavity, the influence of this arrangement on the transducer output was determined by comparison of the transducer output with that of a Bruel and Kjaer type 4136 condenser microphone in an acoustic chamber equipped with a controlled acoustic sound source.

In this arrangement, the amplified oscillator output drove a three-way speaker. The 0.635-cm microphone and the instrumented stator were positioned an equidistance, approximately 200 cm, from the speaker in an anechoic chamber. The sound pressure sensed by the microphone was assumed equal to the pressure on the surface of the instrumented stator and used as a reference to determine the magnitude and phase difference caused by the tube/cavity arrangement. This assumption is valid at low frequencies where the pressure increase caused by the reflection of sound waves from the stator blade and microphone are negligible.

Typical calibration data are shown in Fig. 4. The effects of cavity resonance can be seen, and the response for frequencies greater than about 500-600 Hz may not be accurate due to wave reflection effects. These calibrations indicate a constant frequency response at the wake passing frequencies, approximately 250 Hz, to be encountered in the AFRF.

Presentation of Experimental Data

Using the instrumentation described above, measurements were conducted of the rotor wakes and unsteady pressures on the stator blades. The test variables were: $i = -2$, 5, 17 deg; $R/S = 0.5$ and 2.0 rotor chord lengths; and $\sigma = 0.493$ and 0.986. The following sections describe the data and present some of the typical results obtained. A detailed presentation of the data is given in Ref. 14.

Rotor Wakes

The rotor wakes were measured using a hot-film probe aligned normal to the absolute flow at the stator inlet. Knowing the position of the anemometer, the position of the rotor blades from the once-per-revolution signal, and the absolute flow angle, it was possible to determine the velocity variation as a function of time at the leading edge of the instrumented stator blades.

Figure 5 shows the results of a frequency analysis of typical hot-film wake data obtained at the stator inlet for $R/S = 0.5$ and 2.0 at a constant value of rotor flow coefficient V_x/U. These data show the wakes to be dominated by disturbances at the BPF and its multiples. While a disturbance is visible at 4 and 5 BPF's for $R/S = 0.5$, these harmonics are not visible above the background at $R/S = 2.0$. Also observed was a reduction in the magnitude of the wake deficit with distance downstream of the rotor which is expected due to the wake decay process.

To describe the response of the stator blades to the wakes of the rotor blades, a mean wake was constructed from the ensemble-averaged measurements in one rotor revolution. This was accomplished by breaking the ensemble-averaged data into twelve equal time intervals which were then averaged. This gives an average wake deficit which will change for each stator incidence angle, and rotor-stator spacing. Table 1 presents the maximum nondimensional value of the averaged deficit normal to the stator chord v_d, and the

Table 1 Experimental flow and stator characteristics

σ_s	R/S	α_2	β_2	v_d/V_2	ω
0.493	2.0	−2.0	47.0	0.088	4.97
0.493	2.0	5.0	48.3	0.092	5.22
0.493	2.0	17.0	48.9	0.125	5.33
0.986	2.0	−2.0	47.0	0.086	4.97
0.986	2.0	5.0	48.3	0.089	5.22
0.986	2.0	17.0	48.9	0.083	5.33
0.493	0.5	−2.0	47.0	0.122	4.97
0.493	0.5	5.0	48.3	0.169	5.22
0.493	0.5	17.0	48.9	0.145	5.33
0.986	0.5	−2.0	47.0	0.120	4.97
0.986	0.5	5.0	48.3	0.165	5.22
0.986	0.5	17.0	48.9	0.170	5.33

corresponding reduced frequency based on the stator semichord, $c_s/2$.

Unsteady Stator Blade Pressures

Using the instrumented stators, measurements were made of the unsteady static pressures which occur on both the suction and pressure sides of the blades. The pressure side of the stator was defined as that surface facing the rotor as the rotor moved toward the stator, and the suction surface as the opposite surface (see Fig. 2). This definition means that the circumferential-mean steady flow impinges on the pressure surface at a positive stator incidence angle.

The unsteady pressures recorded at each chordwise position x/c on both the suction and pressure surface were ensemble-averaged. These data were then Fourier-analyzed, and each pressure signal represented as

$$\tilde{p}(t) - p_{\text{atm}} = \sum_{N=1}^{\infty} C_N \cos(nt - \phi_N) \tag{1}$$

where ϕ_N was referenced to the once-per revolution signal. As in the case of the wake data, the predominate harmonics in the transducer signal occurred at BPF and its multiples, i.e., $N = 12,24,36,\ldots$ From this analysis an unsteady pressure coefficient was defined as

$$\tilde{C}_p = \frac{\tilde{p} - p_{\text{atm}}}{\rho v_d V} \tag{2}$$

In order to present the variation of $\tilde{C}_p$ with both time and chordwise position (x/c), the values of $\tilde{C}_p$ were plotted as shown in Fig. 6. This representation shows the variation of $\tilde{C}_p$ during the nondimensional period of time T_0' required for the passage of a single rotor wake from the leading to trailing edge of a blade. At a value of $T_0' = -1.0$, the centerline of a rotor wake occurs at the stator leading edge; when $T_0' = +1.0$, the centerline of the same rotor wake is at the trailing edge of the stator blade. The data of Fig. 6 show that during the passage of a single wake over the stator blade a second wake interacts with the stator. These data permit the examination of the variation of $\tilde{C}_p$ on both the suction and pressure surface as a function of time, x/c, and i for $R/S = 2.0$ and $\sigma = 0.986$.

Two features are evident from the data of Fig. 6. First, the major variations in $\tilde{C}_p$ are observed near the leading edge of the blade, $x/c \leq 0.15$. Second, there is a significant phase shift which occurs between $x/c = 0.02$ and 0.05, i.e., $\tilde{C}_p$ changes from negative to positive values at a fixed time T_0', for $i = 17.0$ deg (Fig. 6b) which is not observed at $i = -2.0$ deg (Fig. 6a). This suggests that the characteristics of the unsteady response of the stator with σ, i, and R/S can be represented by the magnitude of $\tilde{C}_p$ at the leading edge, say $x/c = 0.02$, and the variation of phase angle ϕ_N along the chord. This observation is consistent with other investigators, including Lecort,[15] Satanarayana,[16] Ostdiek,[12] and Fleeter,[17] who observed large pressure variations near the leading edge which decrease rapidly with x/c.

Since the intent of this study was to obtain information regarding the tone noise generated by the existence of unsteady stator pressures at BPF, a logical representation is to consider the difference in $\tilde{C}_p$ and phase angle between the suction and pressure surfaces at BPF, i.e., $N = 12$. Such a representation is accomplished by defining a rms pressure difference coefficient $C_{p_{\text{rms}}}$ as

$$C_{p_{\text{rms}}} = 0.707/\rho v_d V[\,\tfrac{1}{2}(\tilde{p}_{\text{suction}} - \tilde{p}_{\text{pressure}})\ \text{peak-to-peak}\,] \tag{3}$$

and a phase difference at BPF as

$$\Delta\phi_{12} = \phi_{12}(\text{suction}) - \phi_{12}(\text{pressure}) \tag{4}$$

Discussion of Results

For small values of stator incidence angle, $i = -2$ and 5 deg, the variation of $C_{p_{\text{rms}}}$ with x/c is similar and nearly equal (see

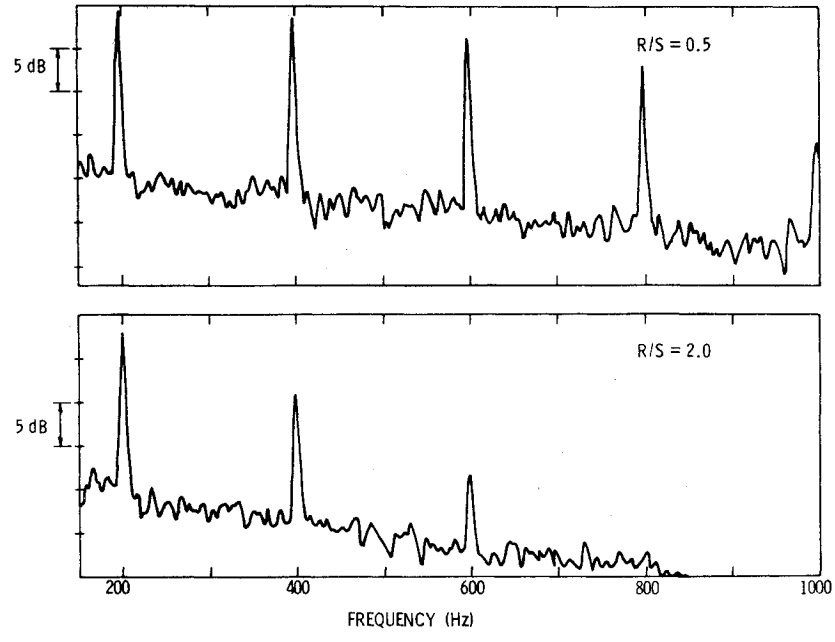

Fig. 5 Typical spectral analysis of hot-film signal.

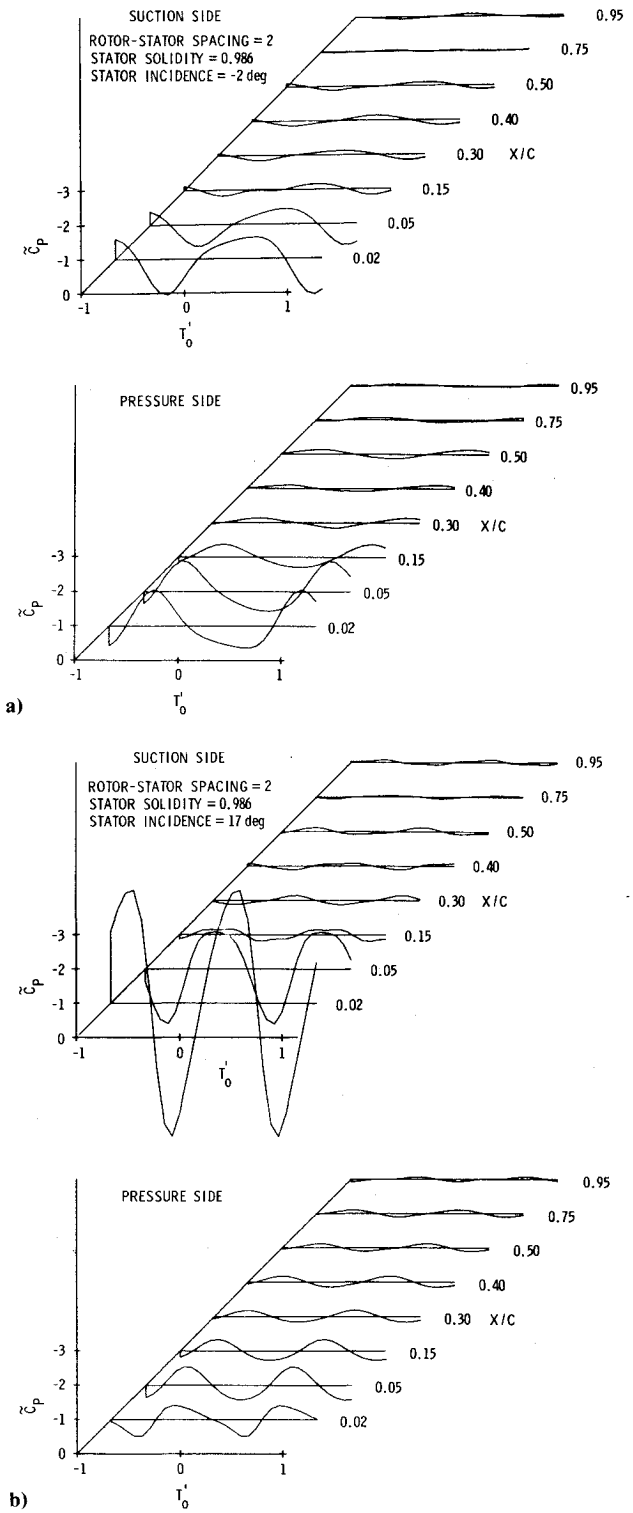

Fig. 6 Unsteady pressure coefficient vs x/c and time. a) $i=-2.0$ deg; b) $i=17$ deg.

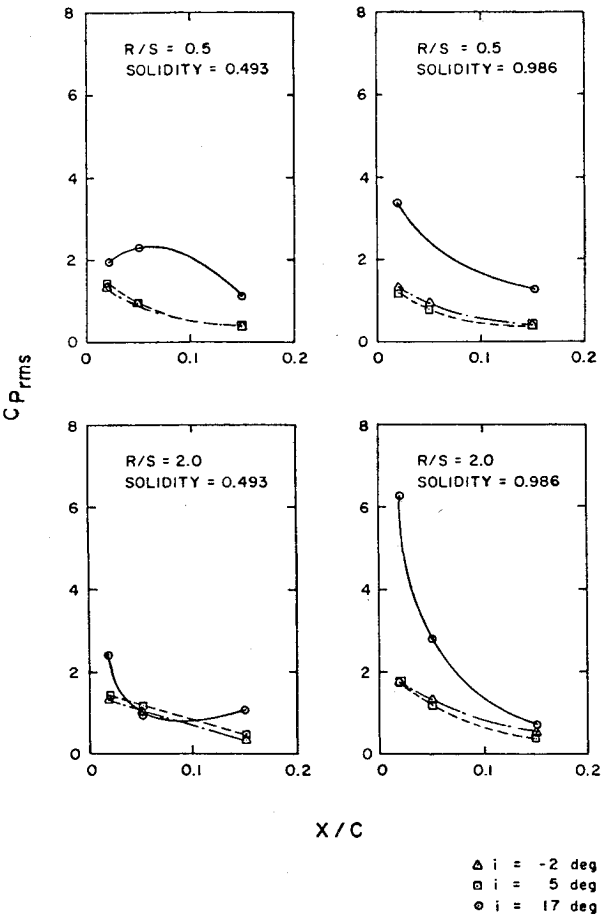

Fig. 7 Variation of $C_{p_{rms}}$ with x/c near leading edge.

Fig. 7). However, at a large value of incidence angle, $i=17$ deg, there is a significant increase in the value of $C_{p_{rms}}$ at a value of $x/c=0.02$ for the higher blade solidity.

Figure 8 is a comparison of the measured and predicted chordwise distribution of $C_{p_{rms}}$ using the unsteady cascade analysis by Smith[10] and the isolated airfoil analysis by Meyer.[8] Both of these analyses assume the airfoils to be flat plates at $i=0$ deg and neglect the effects of airfoil thickness and fluid viscosity. The comparison in Fig. 8 shows that the predicted and measured results exhibit a similar variation with x/c. However, the predicted pressure levels are less than measured because of the assumptions made. The influence of the unsteady cascade interaction is demonstrated by comparison of the cascade and isolated airfoil predictions. However, this difference is expected to be small because of the high value of reduced frequency,[7] $\omega=4.97$.

Figure 9 presents the variation of $C_{p_{rms}}$ at $x/c=0.02$ with incidence angle for constant values of R/S and σ. For the lower value of stator solidity, $\sigma=0.493$, the effect of varying incidence angle from -2 to $+17$ deg has a negligible effect on $C_{p_{rms}}$. However, for $\sigma=0.986$, the incidence angle has a very significant influence on $C_{p_{rms}}$ at the higher value of i.

While there were only two values of solidity investigated, it is possible to show the variation of $C_{p_{rms}}$ with solidity at fixed values of i and R/S (see Fig. 10). The theoretical data by Henderson[7] indicate that for values of $\omega \geq 4.0$ and no steady lift on the blades, there should be little effect of solidity on $C_{p_{rms}}$. The data of Fig. 10 for $i=-2$ and 5 deg confirm this observation. Further, the predicted values of $C_{p_{rms}}$ from the cascade analysis by Smith[10] and the isolated airfoil analysis by Meyer[8] predict a similar trend with solidity. At a value of $i=17$ deg, there is a significant effect of solidity.

Figure 11 presents the measured variation of $C_{p_{rms}}$ as a function of R/S for fixed values of i and σ. The effect of R/S is to alter the maximum wake deficit; v_d will decrease as R/S is increased due to the mixing and diffusion in the wake. The harmonic content of the wake is also affected, but still predominated by $N=12$, i.e., BPF. Since this variation in v_d is included in the definition of $C_{p_{rms}}$, it would be expected that for similar flows over the stators there would be no influence on $C_{p_{rms}}$ due to changes in R/S. This is indeed the result shown in Fig. 11, except for $i=17$ deg and $\sigma=0.986$. Since there were no attempts made to visualize the flowfield over the stators to indicate the existence of local separation, for example, it is impossible to describe these differences.

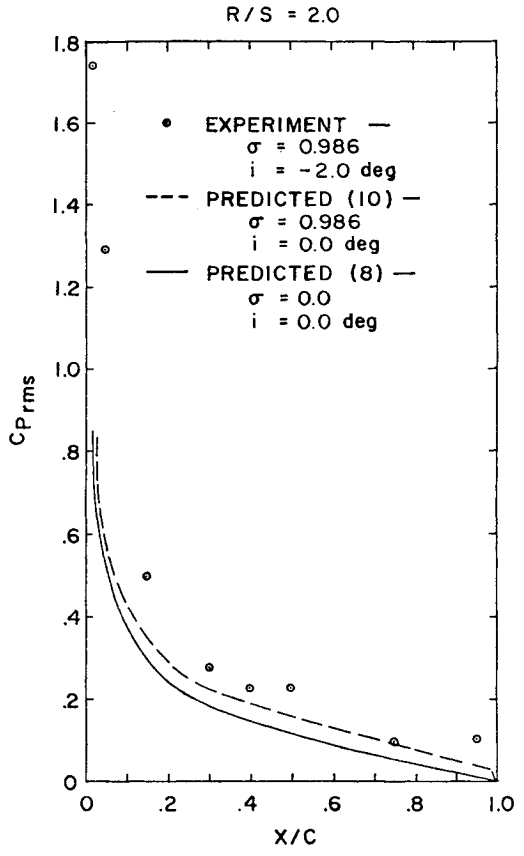

Fig. 8 Comparison of measured and predicted chordwise distribution of $C_{p_{rms}}$.

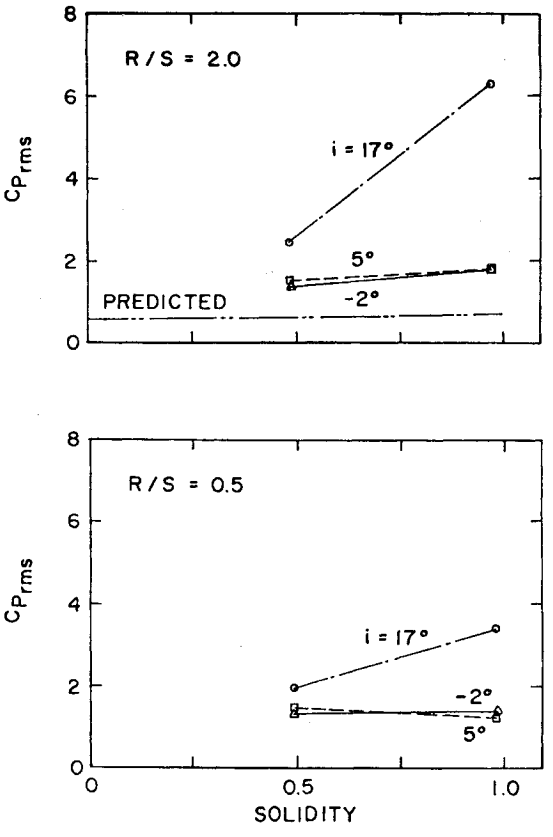

Fig. 10 Variation of $C_{p_{rms}}$ with solidity at $x/c = 0.02$.

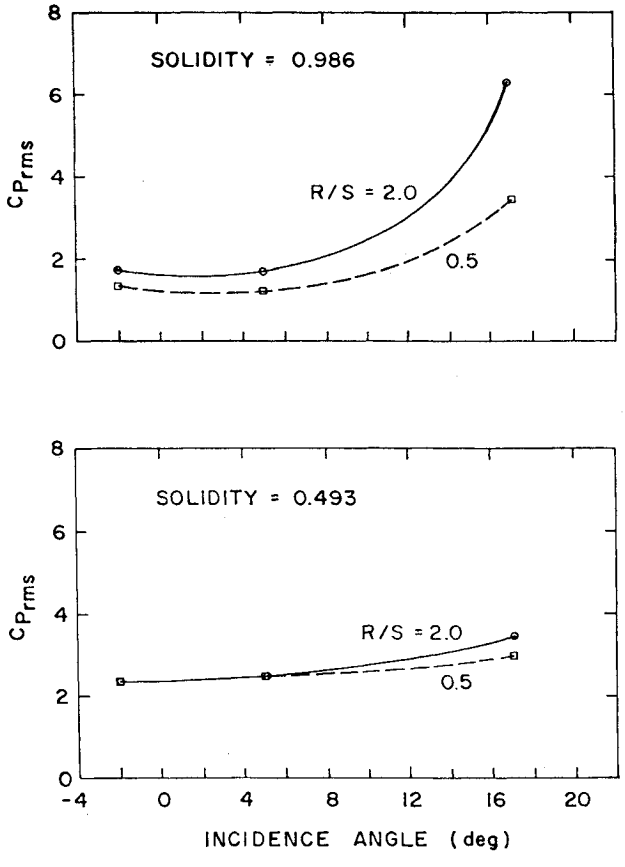

Fig. 9 Variation of $C_{p_{rms}}$ with incidence angle at $x/c = 0.02$.

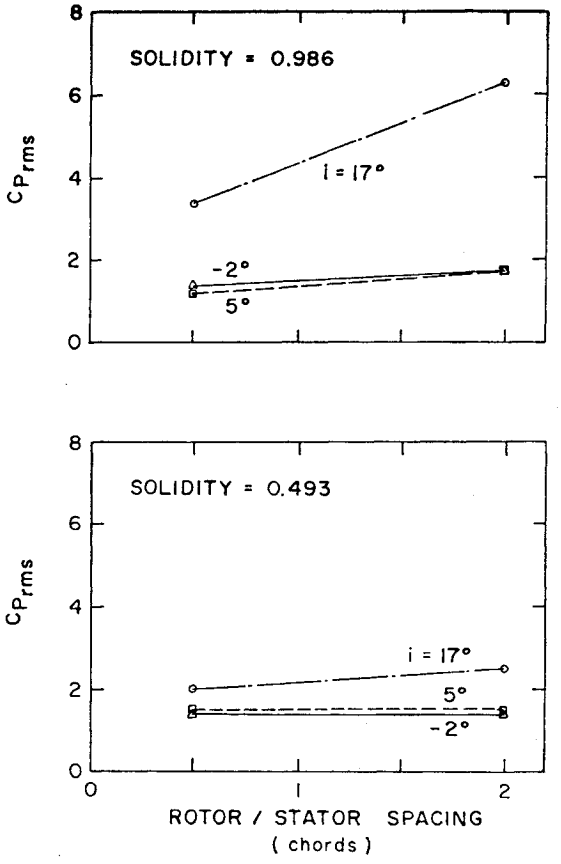

Fig. 11 Variation of $C_{p_{rms}}$ with rotor-stator spacing at $x/c = 0.02$.

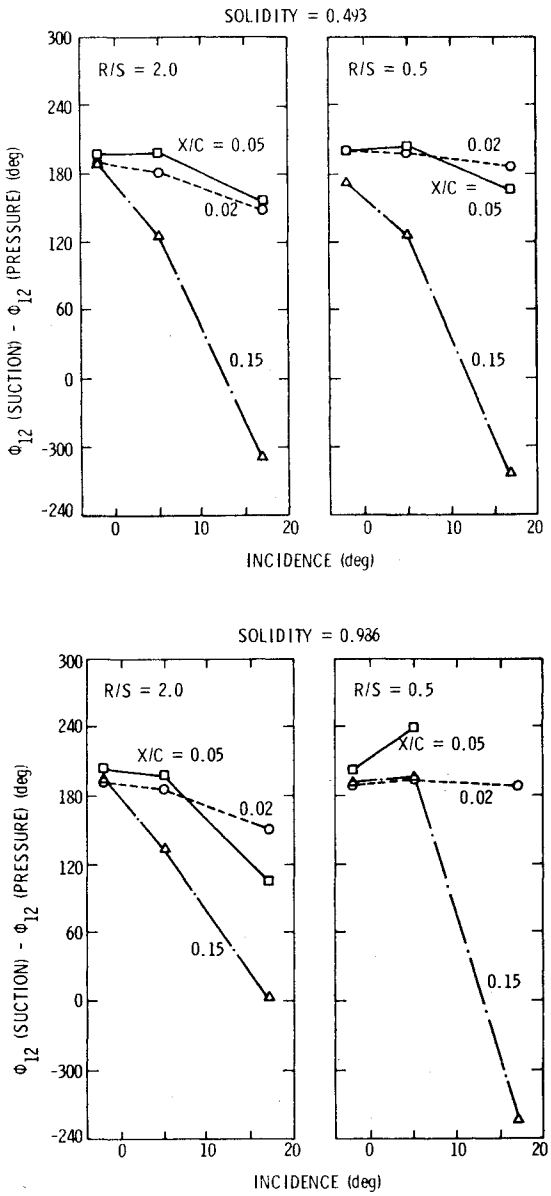

Fig. 12 Variation of phase angle difference at blade passing frequency.

However, Figs. 9 and 10 also indicate that the most significant effects on $C_{p_{rms}}$ occur at $i = 17$ deg and $\sigma = 0.986$.

The question of flow similarity at the different angles of incidence can be partially answered by observing the difference in the phase angle of the unsteady pressures at BPF, ϕ_{12}, referenced to the once-per-revolution timing signal, between the suction and pressure surfaces as a function of x/c and i. Figure 12 presents the difference in ϕ_{12} between the suction and pressure surfaces as a function of i for $x/c \leq 0.15$. These data indicate a significant change in the phase angle difference at $x/c = 0.15$ and $i = 17$ deg. This suggests a different or nonsimilar flow than observed at $x/c = 0.02$ and 0.05 and $i = -2$ and 5 deg. Examination of the pressure traces at $x/c = 0.15$ for $i = 17$ deg (Ref. 14) shows a flattening of the suction side traces at minimum levels of pressure. Other investigators, including Satyanarayana[16] and Carta and St. Hilaire,[18] have also observed this flattening and attribute it to local flow separation.

Summary and Conclusions

The purpose of this study was to investigate the unsteady response of a stator blade to the wakes of an upstream rotor. A portion of this effort was the development of an instrumented stator to allow the measurement of the unsteady pressures on both its pressure and suction sides during such an interaction. This development was successfully completed, and a series of measurements were conducted to demonstrate the effects of rotor-stator spacing, stator solidity, and circumferential time-mean incidence angle on the unsteady pressures on the stator surfaces.

From these unsteady pressure measurements, the following conclusions can be made:

1) While there is an effect on the unsteady stator pressures due to the solidity, this effect is small at the high reduced frequency, $\omega \simeq 5.0$, investigated. The blade-to-blade interactions increase the unsteady pressure difference on the blades as the solidity is increased.

2) The range of rotor-stator spacing investigated has a weak influence on $C_{p_{rms}}$. This indicates only a minor change in the wake characteristics in this range of rotor-stator spacing as long as the flow over the blades is similar, i.e., nonseparated.

3) The difference in phase angle of the unsteady pressure fluctuations on the blade suction and pressure surfaces shows significant variation at high values of incidence angle. It is suspected that this large variation can be attributed to local flow separation.

Several observations can be made concerning the theoretical prediction of the unsteady pressure difference:

1) The prediction of the distribution of the unsteady pressure difference by both an isolated airfoil and a cascade analysis results in a distribution with x/c which is similar to the measured distribution, but with lower magnitudes of pressure difference.

2) The comparison of the isolated airfoil and cascade analyses shows the effect of the unsteady blade-to-blade interaction. While for the high values of reduced frequency considered in this program this interaction is small, other theoretical analyses indicate this interaction to be much larger at lower values of ω.

3) The assumption in the analyses that the unsteady pressures on opposite sides of the blades are 180 deg out-of-phase is valid only at low values of incidence and near the leading edge of the blades.

Acknowledgments

This study was conducted under the primary sponsorship of NASA Research Grant No. NGR 39-009-275, Lewis Research Center. The administration of this grant was conducted through the Department of Mechanical Engineering of The Pennsylvania State University. Partial support was provided by the U.S. Navy, Naval Sea Systems Command, Code 63R3 through the Applied Research Laboratory of The Pennsylvania State University which made available the facilities used in this study.

References

[1] Feiler, C.E. and Conrad, E.W., "Fan Noise from Turbofan Engines," *Journal of Aircraft*, Vol. 13, Feb. 1975, pp. 128-134.

[2] Dittmar, J.H., "Methods for Reducing Blade Passing Frequency Noise Generated by Rotor-Wake Stator Interaction," NASA TM X-2669, Nov. 1972.

[3] Sears, W.R., "Some Aspects of Non-Stationary Airfoil Theory and Its Practical Application," *Journal of Aeronautical Sciences*, Vol. 8, No. 3, Jan. 1941, pp. 104-108.

[4] Horlock, J.H., "Fluctuating Lift Forces on Aerofoils Moving through Transverse and Chordwise Gusts," *ASME Journal of Basic Engineering*, Vol. 90, No. 4, Dec. 1968, pp. 478-483.

[5] Dittmar, J.H. and Woodward, R.P., "Fan Stage Redesigned to Decrease Stator Lift Fluctuation Noise," *Journal of Aircraft*, Vol. 14, Aug. 1977, pp. 746-750.

[6] Goldstein, M. and Attasi, H., "A Complete Second-Order Theory for the Unsteady Flow about an Airfoil Due to a Periodic Gust," *Journal of Fluid Mechanics*, Vol. 74, Part 4, April 1976, pp. 741-765.

[7] Henderson, R.E., "The Unsteady Design of Axial-Flow Turbomachines," *Proceedings of ASME/IAHR/ASCE Symposium on Fluid Machinery*, Fort Collins, Col., Vol. 2, June 1978, pp. 91-108.

[8] Meyer, R.X., "The Effect of Wakes on the Transient Pressure and Velocity Distributions in Turbomachines," *ASME Transactions*, Vol. 80, Oct. 1958, pp. 1544-1552.

[9] Whitehead, D.S., "Force and Moment Coefficients for Vibrating Aerofoils in Cascade," Aeronautical Research Council R and M 3254, Feb. 1960.

[10] Smith, S.M., "Discrete Frequency Sound Generation in Axial Flow Turbomachines," Aeronautical Research Council R and M 3709, 1973.

[11] Satyanarayana, B., "Some Aspects of Unsteady Flow Past Airfoils and Cascades," *Unsteady Phenomena in Turbomachinery*, AGARD Conference Proceedings No. 177, April 1976, pp. 25-1 to 25-11.

[12] Ostdiek, F.R., "A Cascade in Unsteady Flow," *Unsteady Phenomena in Turbomachinery, AGARD Conference Proceedings No. 177*, April 1976, pp. 26-1 to 26-13.

[13] Bruce, E.P. "The ARL Axial Flow Research Fan—A New Facility for Investigation of Time-Dependent Turbomachinery Flows," ASME Paper 74-FE-27, Joint Fluids Engineering and CSME Conference, Montreal, Canada, May 1974.

[14] Henderson, R.E. and Franke, G.F., "Investigation of the Unsteady Pressure Distribution on the Blades of an Axial Flow Fan," Applied Research Laboratory, The Pennsylvania State University, Tech Memo TM 78-54, 1978.

[15] Lefcort, M.D., "An Investigation into Unsteady Blade Forces in Turbomachines," *ASME Journal of Engineering for Power*, Vol. 87A, 1965, pp. 345-354.

[16] Satyanarayana, B., "Unsteady Flow Past Aerofoils and Cascades," Ph.D. Dissertation, Wolfson College, University of Cambridge, 1975.

[17] Fleeter, S., Jay, R.L., and Bennett, W.A., "Rotor Wake Generated Unsteady Aerodynamic Response of a Compressor Stator," ASME Paper 78-GT-112, International Gas Turbine Conference, London, England, April 1978.

[18] Carta, F.O. and St. Hilaire, A.O., "Experimentally Determined Stability Parameters of a Subsonic Cascade Oscillating near Stall," *ASME Journal of Engineering for Power*, Vol. 100, No. 1, Jan. 1978, pp. 111-120.